J Mater Sci (2012) 47:625–631
DOI 10.1007/s10853-011-5831-y

Glass transition and fragility of telluro-vanadate glasses containing antimony oxide

Dariush Souri

Received: 31 May 2011 / Accepted: 28 July 2011 / Published online: 10 August 2011

Abstract The activation energy (ΔH^*) of the glass transition and the heating-rate dependence of the glass transition temperature (T_g) of V_2O_5–Sb_2O_3–TeO_2 glasses were determined using differential scanning calorimetry technique. Non-isothermal measurements were performed at different heating rates φ (=3, 6, 9, 10, 13 K/min). The heating rate dependence of T_g was used to investigate the applicability of different theoretical models describing the glass transition. The application of Moynihan and Kissinger et al. models to the present data led to different values of (ΔH^*) at each different heating-rate regions. This behavior was attributed to the strong heating rate dependence of the activation energy of the process. The fragility parameter ($m = \Delta H^*/RT_g$) were $\lesssim 90$, suggesting that these glasses may be classified as strong glasses. The viscosity, η, calculated at a few selected temperatures near the glass transition region increased with increasing Sb_2O_3 content at any given temperature, which is also expected. Also the compositional dependence of T_g and ΔH^* was investigated.

Introduction

An understanding of the structure and physical properties of the tellurium-based glasses is important because of the technical, scientific, and technological interest of these glasses [1–15]. Study in structural characteristics of glasses by spectral analyzing and differential scanning calorimetry (DSC) curve can be a suitable way to understand the behavior of glasses [16]. The glass transition and associated anomaly of relaxation behavior are the subject of many theoretical and experimental investigations [17–19]. In spite of extensive research devoted to understand the phenomenon of glass transition, there is no satisfactory description of this phenomenon and more work is needed to overcome this difficulty. The DSC technique is widely used to investigate the glass transformation in glassy materials. The kinetics of the glass transition as studied by the DSC method is important in investigating the nature the glass transformation process. Moreover, the kinetic aspect of the glass transition is evident from the dependence of T_g on the heating rate. This behavior can be used to identify different mechanisms involved in the transition process. One of the key kinetic parameters which can be determined by DSC measurements is the activation energy, ΔH^*, of the glass transition. ΔH^* can be determined from the dependence of T_g on heating rate [20]. Glasses, which strongly resist any structural changes with changing temperature, are characterized as strong glasses [21–23]. Consequently, the strong glasses show only a small change in heat capacity in the glass transition region. In contrast, the glasses, whose structures undergo a large change with changing temperature and which show a large change in heat capacity in the glass transition region, are referred to as fragile glasses. In classifying strong–fragile characteristics for glasses, Angell used [21] a log viscosity (η) versus reduced temperature (T_g/T, T_g being the glass transition temperature) plot such as one shown schematically in Fig. 1.

Strong glasses [22, 23] have a highly polymerized, mostly covalently bonded, network and the temperature dependence of η near the glass transition region for such liquids is nearly Arrhenian (log η vs. $1/T$ plot is linear). For

D. Souri (✉)
Department of Physics, Faculty of Science, Malayer University, Malayer, Iran
e-mail: d.souri@gmail.com; d.souri@malayeru.ac.ir

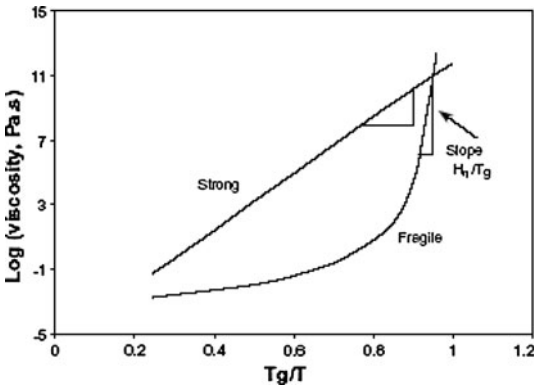

Fig. 1 Schematic plot of temperature dependence of log(viscosity) for "strong" and "fragile" glasses [21]

fragile glasses (Chalcogenide [24–27], iron phosphate [28]), whose network is ionic or molecular type, the temperature dependence of viscosity is typically non-Arrehenian, and the log η versus $1/T$ plots for these liquids deviate from linearity. The slope at any point on the curves in Fig. 1 yields the value for $\Delta H_\eta/T_g$, where ΔH_η is the activation energy for viscous flow. Thus, for strong glasses, $\Delta H_\eta/T_g$ is nearly constant with temperature near the glass transition region, but it is temperature dependent and increases rapidly with decreasing temperature near the glass transition region for typical fragile glasses. The fragile glasses are characterized generally by a high value of $\Delta H_\eta/T_g$. For most glass forming liquids the activation energy for glass transition, ΔH^*, is indistinguishable from ΔH_η near the glass transition region [25, 26]. Thus, measuring and evaluating the values for ΔH^* are often used to determine the strong–fragile characters of glasses [25, 26].

To the best of our knowledge, there are some articles on the calorimetric, structural, and elastic properties of multicomponent TeO_2- or V_2O_5-based glasses [5, 7, 8, 10]. For the present samples (V_2O_5–Sb_2O_3–TeO_2), beside the some optical properties, calorimetric properties such as glass transition temperature and crystallization temperature have been previously reported only at heating rate $\varphi = 10$ K/min [6]; as addressed in continue, in this study, attention is focused on the fragility parameter and also the effect of different heating rates on the thermal characters. This study reports the glass transition behavior for V_2O_5–Sb_2O_3–TeO_2 oxide glasses with the purpose of (1) evaluating their strong/fragile character, which is related to the degree of structural reorganization with temperature near the glass transition region, (2) to investigate the effect of heating rate on the glass transition, (3) to investigate the variation of the activation energy of the glass transition, (4) to use the experimental data to test a number of theoretical models proposed to describe the glass transition, and (5) to calculate the viscosity about glass transition region.

Experimental procedure

The ternary $(60 - x)V_2O_5$–$40TeO_2$–xSb_2O_3 glasses with $0 \leq x \leq 10$ (in mol%), hereafter termed as 40TVSx, were prepared by standard melt quenching technique; the melting temperature of the present samples was in the range 680–750 °C, and show increasing trend with increasing of antimony oxide content. During the sample production, the melt was mixed every 5 min to prevent the separation of the three components. The melt was poured on to a polished steel block and immediately pressed by another polished steel block, where the blocks were kept at room temperature. All of the obtained bulk samples were annealed at 473 K for 2 h to eliminate the mechanical stresses resulting from the quenching. The characterization of the glass systems was carried out by X-ray diffraction (XRD) studies using a Bruker diffractometer (AXS D8 Advance, Cu K_α, Germany). The density (ρ) of each sample was calculated by the Archimedes's method using para-xylene as immersion liquid; results of density, XRD patterns, and glass transition temperature have been previously reported [6]. Also, the glass transition temperature (T_g) of these samples were obtained using DSC (NETZSCH DSC 200 F3, Germany) under dynamic N_2 gas atmosphere (at a constant rate of 30 cm^3/min); for each DSC measurement, the sample was first heated at an arbitrary heating rate (normally 20 K/min) to a temperature that is 20–30 K higher than its glass transition temperature (T_g) and held there for 5 min to erase the previous thermal history (during cooling the melt) of the glass. After the isothermal hold, the sample was cooled at 6 K/min through the glass transition region to a temperature ($\sim$100 °C) well below T_g, and then reheated at a rate (φ) of 3, 6, 9, 10, and 13 K/min to obtain the DSC curves.

Results and discussion

XRD patterns

XRD characterization of 40TVSx samples has been carried out on different samples, confirming the amorphous nature of them; results have been reported in our previous study [6].

Thermal analysis and activation energy for glass transition (ΔH^*)

The representative DSC plots of the 40TVS0 sample recorded at different heating rates are shown in Fig. 2. The measured data for other samples are presented in Table 1.

In the absence of thermal events, the position of the baseline in such a plot is proportional to the specific heat of

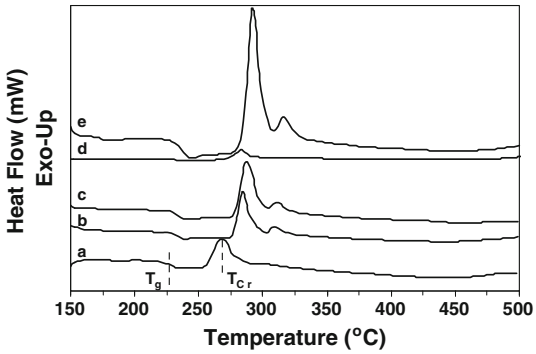

Fig. 2 DSC curves of the 40TVS0 sample at different heating rates *a* $\varphi = 3$ K/min, *b* $\varphi = 6$ K/min, *c* $\varphi = 9$ K/min, *d* $\varphi = 10$ K/min, *e* $\varphi = 13$ K/min

the sample. The presence of an endothermic peak, superimposed on the baseline, indicates the occurrence of a heat-absorbing event such as glass transition or melting. On the other hand, an exothermic peak occurs as a result of some sort of heat-releasing event such as crystallization [29]. The structural transformation is characterized by two temperatures T_g, T_{cr}. The glass transition temperature, T_g, as defined by the endothermic change in the DSC trace indicates a large change of viscosity, marking a transformation from amorphous solid phase to supercooled liquid state. As the output of the DSC during heating is proportional to the heat capacity, it is a straightforward and convenient method of detecting the glass transition and investigating its kinetics. For example, the heating-rate dependence of the glass transition temperature T_g can be used to determine the activation energy of the transition from glassy to liquid state [19, 20, 29, 30]. In this study, the middle point of the endothermic trace was used to define T_g. Other definitions for T_g were used by different authors. For instance, Abu-Sehly et al. [20] and Moynihan et al. [26] used different definitions of T_g that included the extrapolated onset, the inflection point and the maximum point of the endothermic trace. Using these definitions of T_g, the result of extracting the activation energy for different glasses was found to be the same. In Table 1, the data of T_g and T_{cr} at heating rate 10 K/min have been reported in our previously article [6].

The exothermic peak temperature T_{cr} is used to identify the crystallization process. As listed in Table 1, both T_{cr} and T_g shift to higher temperatures with increasing heating rate. The heating-rate dependence of T_g is clearly indicated in the Fig. 2 and Table 1. The kinetic aspect of the glass transition is evident from the pronounced shift in T_g. It is worth observing that an order of magnitude increase in φ causes a shift in T_g of 5 K.

It has been widely observed that the dependence of the T_g on the heating-rate φ follows Lasocka's formula [31]:

$$T_g = a + b\ln\varphi, \quad (1)$$

where a and b are constants for a given glass composition. In order to see if Eq. 1 describes the heating-rate dependence of T_g, the T_g is plotted against $\ln\varphi$ as shown in Fig. 3 representatively for 40TVS0 sample. As evident from this figure, the present data cannot be fitted to Eq. 1 for the whole range of φ and there are two different linear regions.

Table 1 Activation energy for glass transition ΔH^* determined using Eqs. 2 and 3 at lower and higher heating rate regions, fragility (m) at lower heating rates, glass transition temperature (T_g) and crystallization temperature (T_{cr}) for 40TVSx glasses at the different heating rates (φ)

Glass	Φ (K/min)	T_g (°C)	T_{cr} (°C)	m	ΔH^* (kJ/mol) at lower φ	ΔH^* (kJ/mol) at higher φ
40TVS0	3	227.70	267.16	69.71	From Eq. 2: 293	From Eq. 2: 506
	6	232.68	283.20		From Eq. 3: 284	From Eq.3: 497
	9	234.40	286.80			
	10	234.80	287.50			
	13	235.96	290.64			
40TVS5	6	256.70	354	49.23	From Eq. 2: 216	From Eq. 2: 269
	9	261.10	364.10		From Eq. 3: 208	From Eq. 3: 260
	10	261.60	365.60			
	13	264.20	383			
40TVS8	3	269.60	397.60	87.43	From Eq. 2: 397	From Eq. 2: 132
	6	274.10	421.70		From Eq. 3: 388	From Eq. 3: 123
	9	276.40	438.80			
	10	277.50	444.10			
	13	281.60	449.60			
40TVS10	3	273.91	423.11	66.78	From Eq. 2: 306	From Eq. 2: 549
	6	278.52	448.52		From Eq. 3: 297	From Eq. 3: 540
	9	283	474.27			
	10	283.67	383.10			
	13	284.75	385.72			

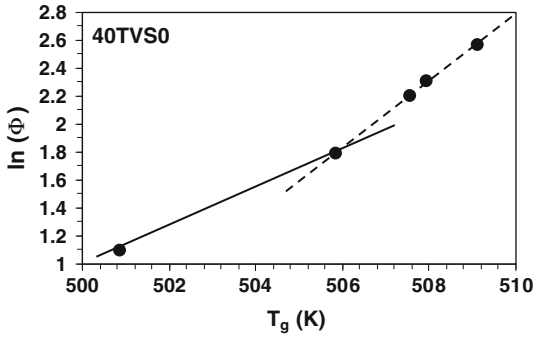

Fig. 3 Representative plot of lnφ against the glass transition temperature T_g. The *solid* and *dashed lines* represent fit to Eq. 1 at different heating rate regions, which imply to strongly temperature dependence of activation energy; *straight lines* are drawn for the guide for eye to distinct the different heating rate regions

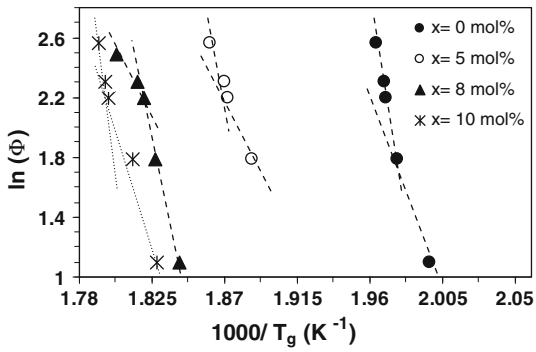

Fig. 4 Plots of lnφ versus $1000/T_g$ (Eq. 2) for 40TVSx glasses; *straight lines* are drawn for the guide for eye to distinct the different heating rate regions, and the slopes are equal to $(-\Delta H^*/1000\ R)$

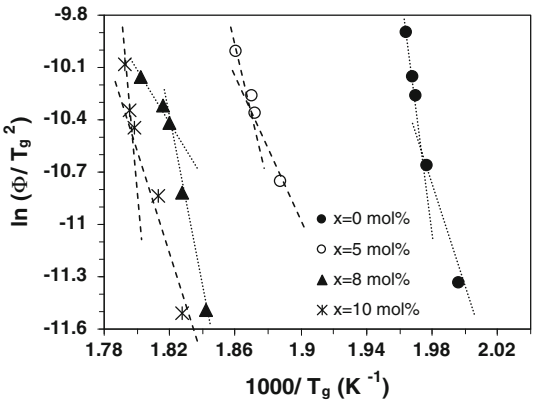

Fig. 5 Plots of $\ln[\varphi/T_g^2]$ versus $1000/T_g$ (Eq. 3) for 40TVSx glasses; *straight lines* are drawn for the guide for eye to distinct the different heating rate regions, and the slopes are equal to $(-\Delta H^*/1000\ R)$

As pointed out by Mehta et al. [32], the values of a and b are sensitive to the cooling rate of the melt. This behavior indicates that the physical significance of a and b is related to the nature of the structural relaxation within the glass transition region. It is evident from Fig. 3 that the values of a and b are different for different heating rate regions; these different values of a and b obtained in this study may be related to a change in the transformation processes involved in the glass transition.

Based on structural relaxation models, the heating and cooling rate dependence of the glass transition temperature was investigated by many authors [26, 33–36]. The model frequently used to determine the activation energy (ΔH^*) for structural relaxation in the glass transition region is given by Moynihan [25] as:

$$\mathrm{Ln}\varphi = -\Delta H^*/(RT_g) + \text{constant}, \tag{2}$$

where T_g is the glass transition temperature determined from the DSC curve measured at a heating rate of φ and R is the gas constant.

The value of ΔH^* is determined from the slope of the plots, lnφ versus $1/T_g$.

On the other hand, a Kissinger-type equation [37], which is generally used to determine the activation energy for structural relaxation, is also used to determine ΔH^* and is given by:

$$\left[\ln\left(\varphi/T_g^2\right)\right] = \left(-\Delta H^*/T_g R\right) + \text{constant}. \tag{3}$$

Thus, the slope of the $\ln(\varphi/T_g^2)$ versus $1/T_g$ plot gives the value for ΔH^*.

Both types of plots, $\ln(\varphi)$ versus $1/T_g$ (Eq. 2) and $\ln(\varphi/T_g^2)$ versus $1/T_g$ (Eq. 3), for the present glasses show, as expected, linear relationship with a linear correlation factor better than 0.9987. Such plots are shown in Figs. 4 and 5 for 40TVSx glasses. Furthermore, as is evident from Figs. 4 and 5, two regions can be identified in the plots. This leads to two different values for the activation energy in each heating rate region; the obtained data of ΔH^* are listed in Table 1; for example in the case of 40TVS0 sample upon the Moynihan model (Eq. 2), In the low-φ region, the activation energy for the glass transition is 293 kJ/mol and in the high-φ region the activation energy is 506 kJ/mol; on the other hand, upon the Kissinger et al. model (Eq. 3), In the low-φ region, the activation energy for the glass transition is 284 kJ/mol and in the high-φ region the activation energy is 497 kJ/mol for the same sample. This deviation (existence of two φ-regions) from Moynihan or Kissinger et al. predictions shows that the glass transition process cannot be described by constant activation energy. As will be shown below this behavior is attributed to the rather strong heating-rate dependence of the activation energy in the present sample. It is worth mentioning that although Moynihan and Kissinger equations are based on different theoretical models, they both led to similar values of the activation energies in the lower and higher heating rate regions, which suggests that both equations are useful in determining ΔH^*; However, the

ΔH^* values from Eq. 2, on the average, 8–10 kJ/mol differs from those from Eq. 3. It should be mentioned here that the above analysis showed that even on the basis of Moynihan and Kissinger models, the process of glass transition cannot be described by single activation energy. As will be shown below this behavior was found to be a consequence of a strong heating-rate dependence of the activation energy. It is therefore tempting to investigate the dependence of the glass transition activation energy on the heating rates; so, the values of ΔH^* determined from the slope of such straight lines are given in Table 1 and is shown in Fig. 6 as a function of glass composition.

Table 1 and Fig. 6 show that ΔH^* for the present glasses has a steep change at $x = 8$ mol%, in both heating rate region. For example, at lower φ-region, 40TVS8 has the highest ΔH^* equal to 506 kJ/mol; as reported in my previous study [6], also optical gap and molar volume have a sharp change for this sample as a consequence of increasing the concentration of non-bridging oxygens (NBOs), which means the structural change in the system 40TVSx at $x = 8$ mol%. The increase of NBO's means the increasing of fragility of the glass as can be seen in the fragility evaluating.

On the other hand, the DSC data reported at Table 1 show that for the different compositions of the system at different heating rates, the glass transition temperature increase with increasing antimony oxide content and all the other heating rates indicate similar behavior. This variation is shown in Fig. 7, where T_g is seen to increase with increasing x or with decreasing V-content for each heating rate. Furthermore, using the results of our previous study [6] and results presented in Fig. 7, T_g data show that the glass transition temperature is sensitive to the Sb_2O_3 concentration; in other word, in this study, the change in T_g indicates a change related to the manner in which V_2O_5 and Sb_2O_3 get arranged in the glass; also the glass transition temperature increases if the average coordination number increases. This may be due to the decrease in the number of V–O–V bonds and the increase of the V–O–Sb bonds as a result of the increasing of the Sb_2O_3 content (x) and the decrease of the V content. In other words, the cross-linking provided by Sb atoms increases for 40TVSx samples, which in turn affects the structure in a manner to increase the T_g; now, no FTIR spectra are available to clarify the structural information.

A parameter, m, known as the "fragility parameter" and defined [38] as $m = \frac{\Delta H^*}{RT_g}$ was calculated and plotted as a function of composition in Fig. 8, see also Table 1, which has a step change at $x = 8$ mol% as discussed previously; the calculated m values for 40TVSx glasses are in the range 49–88.

Although there is no sharp limit to determine strong–fragile characters of glasses on the basis of m values, a value of $m \lesssim 90$ is typical of strong glasses [39]. Thus, upon this criterion, the present glasses are suggested to be strong and have good resistance against thermal shocks and so are probably suitable candidates for technological applications. Generally, glasses with higher thermal stability have higher resistance against heat shocks and therefore have lower fragility; on the other hand, thermal stability depends on $\Delta T = T_{cr} - T_g$ [7]; thus, it can be concluded from the data reported in Table 1, that ΔT increase from ~ 50 (for 40TVS0) to ~ 103 (for

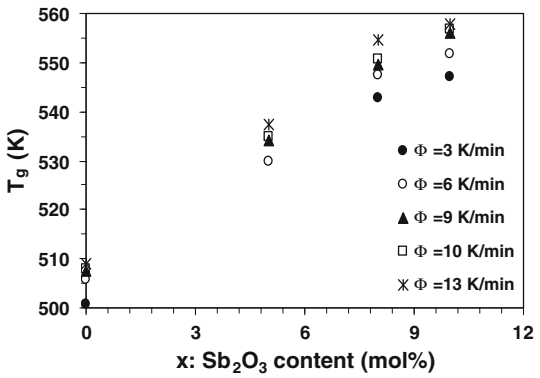

Fig. 7 Variation of T_g with antimony oxide concentration (x) at different heating rates

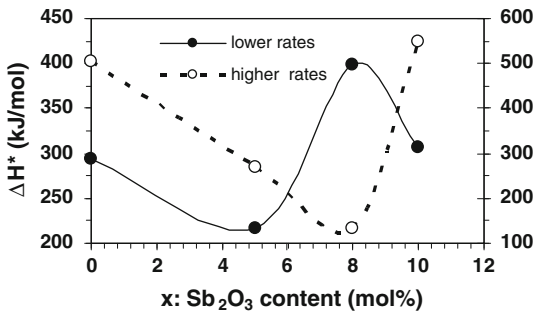

Fig. 6 Plot of ΔH^* against antimony oxide content (x) at different φ-regions, for 40TVSx glasses

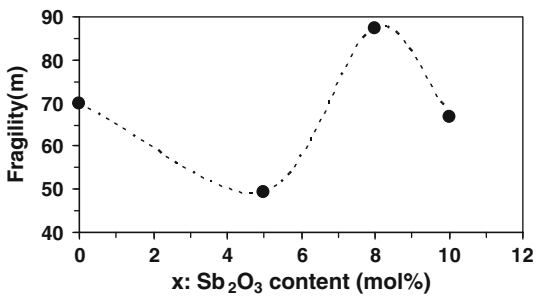

Fig. 8 Variation of fragility parameter with Sb_2O_3 content, for 40TVSx glasses

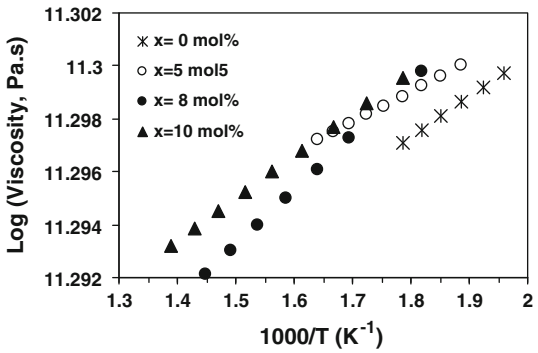

Fig. 9 Calculated viscosity as a function of 1000/T in the glass transition region for 40TVSx glasses (logarithmic function on the y-axis is in the base 10)

40TVS5). So, fragility (m) and then ΔH^* decrease abruptly for the sample with $x = 5$ mol% antimony oxide.

Finally, it is known [40, 41] that TeO_4 triangular bipyramidal (tbp) units present in crystalline TeO_2 transform to TeO_3 triangular pyramids (tp) in some glasses. With the addition of Sb_2O_3 in 40TVSx system, the transformation of tbps to tps may occur and therefore is associated with the formation of NBOs, which introduce weaker bonds in the glass network. Thus, increasing of Sb_2O_3 in a glass makes the glass network less strong, which is manifested an increasing fragility (m) of the glass; this interpretation can be realized from the variations of m and ΔH^*, as discussed previously. Now, no FTIR spectra are available to justify this result.

Viscosity in the glass transition region

It has been shown [25, 26, 42] that the viscosity of a glass, η, at any temperature, T, near the glass transition region can be calculated with a reasonable accuracy from the glass transition temperature, T_g, and activation enthalpy for glass transition, ΔH^*, using the relation:

$$\mathrm{Log}\,\eta(\mathrm{T}) = 11.3 + (\Delta H^*/2.3R)[(1/T) - (1/T_g)]. \quad (4)$$

The viscosity for the present tellurite glasses was calculated (Eq. 4) at a few selected temperatures above T_g and is shown as a function of temperature in Fig. 9.

The value of T_g obtained from the heat capacity curve at a heating rate of 6 K/min for each glass was used in these calculations. As shown in Fig. 6, the viscosity at any given temperature for these glasses increases with increasing antimony oxide content, which is expected. There is no experimental data currently available for these glasses with which the calculated values of viscosity (Fig. 9) can be directly compared.

The glass transition temperature (T_g) for the present glasses increases with increasing Sb_2O_3 content (see Table 1), which is expected.

Conclusions

Investigation of heating-rate dependence of the glass transition temperature in $(60 - x)V_2O_5$–$40TeO_2$–xSb_2O_3 glasses was carried out using DSC technique. It was observed that T_g shifted to higher temperatures with increasing of heating rates. The observed dependence was discussed in terms of different theoretical models describing glass transition. It was shown in this study that the transition process cannot be described in terms of single activation energy. This study shows the assumption that the glass activation energy does not vary during the glass transition process is not valid. The activation energy ΔH^* and fragility m were determined for the present glasses. The calculated viscosity at any temperature in the glass transition region increased with increasing Sb_2O_3 content, as expected. The fragility characteristics of these glasses, has a sharp change at $x = 8$ mol%, which is in accordance with the variations of ΔH^* and molar volume. Generally, these glasses are in the strong glass category and probably are good candidates for fabrication because they have good resistance against thermal shocks.

References

1. Burger H, Vogel W, Kozhukharov V (1985) Infrared Phys 25:395
2. Kim SH, Yoko T, Sakka S (1993) J Am Ceram Soc 76:2486
3. Yoko T, Kamiya K, Yamada H, Tanaka K (1988) J Am Ceram Soc 71:C70
4. Stanworth JE (1952) J Soc Glass Technol 36:217
5. Luo S, Xu W, Zhang X, Huo L (2011) Mat Sci Forum 663–665:1229
6. Souri D, Shomalian K (2009) J Non Cryst Solids 355:1597
7. Prashant Kumar M, Sankarappa T, Awasthi AM (2008) Physica B 403:4088
8. Taibi Y, Poulain M, Lebullenger R, Atoui L, Legouera M (2009) J Optoelectron Adv Mater 11:34
9. Souri D, Elahi M (2007) Phys Scr 75(2):219
10. Rada M, Maties V, Rada S, Culea E (2010) J Non Cryst Solids 356:1267
11. Chowdari BVR, Kumari PP (1997) J Phys Chem Solids 58(3):515
12. Pal M, Hirota K, Tsujigami Y, Sakata H (2001) J Phys D Appl Phys 34:459
13. Sharma BK, Dube DC, Mansingh A (1984) J Non Cryst Solids 65:39
14. Murugan GS, Ohishi Y (2004) J Non Cryst Solids 341:86
15. Jayaseelan S, Muralidharan P, Venkateswarlu M, Satyanarayana N (2005) Mater Sci Eng B 118:136
16. Turky G, Dawy M (2002) Mater Chem Phys 77:48
17. Elliott SR (1990) Physics of amorphous materials, 2nd edn. Longman Scientific & Technical, Essex
18. Scherer GW (1986) Relaxation in glasses and composites. Wiley, New York
19. Avramov I, Guinev G, Rodrigues ACM (2000) J Non Cryst Solids 271:12
20. Abu-Sehly AA, Abu El-Oyoun M, Elabbar AA (2008) Thermochim Acta 472:25

21. Angell CA (1988) J Phys Chem Solids 49:863
22. Angell CA (1985) J Non Cryst Solids 73:1
23. Angell CA (1991) J Non Cryst Solids 131–133:13
24. Kasap SO, Yannacopoulos S (1989) J Mater Res 4:893
25. Moynihan CT (1993) J Am Ceram Soc 76:1081
26. Moynihan CT, Easteal AJ, Wilder J, Tucker J (1974) J Phys Chem 78:2673
27. Moynihan CT, Easteal AJ, Tran DC, Wilder JA, Donovan EP (1976) J Am Ceram Soc 59:137
28. Fang X (2000) PhD thesis, Ceramic Engineering Department, University of Missouri-Rolla
29. Smith GW, Pinkerton FE, Moleski JJ (1999) Thermochim Acta 342:31
30. Vyazovkin S, Sbirrazzuoli N, Dranca I (2004) Macromol Rapid Commun 25:1708
31. Lasocka M (1976) Mater Sci Eng 23:173
32. Mehta N, Shukla RK, Kumar A (2004) Chalcogenide Lett 1:131
33. Ritland H (1956) J Am Ceram Soc 39:403
34. Avramov I (1996) Thermochim Acta 280:363
35. Avramov I, Avramova N (1999) J Non Cryst Solids 260:15
36. Yue Y (2004) J Chem Phys 120:8053
37. Kissinger HE (1956) J Res Natl Bur Stand (US) 57:217
38. Bruning R, Sutton M (1996) J Non Cryst Solids 205–207:480
39. Lee SK, Tatsumisago M, Minami T (1994) Phys Chem Glasses 35:226
40. Komatsu T, Noguchi T (1997) J Am Ceram Soc 80:1327
41. Komatsu T, Noguchi T, Benino Y (1997) J Non Cryst Solids 222:206
42. Zhu D, Ray CS, Zhou W, Day DE (2003) J Non Cryst Solids 319:247